

Optimization of Convolutional Neural Networks for Detecting Oral Cancer-Induced Bone Invasion: A Genetic Algorithm Approach

Pinky Agarwal¹, Arya Kale², Anju Yadav³, Pratistha Mathur⁴

¹Computer Applications, Manipal University Jaipur, Dehmi Kalan, Jaipur, 303007, Rajasthan, India

^{2,3,4}Information Technology, Manipal University Jaipur, Dehmi Kalan, Jaipur, 303007, Rajasthan, India

Article History:

Received: 08-09-2024

Revised: 27-10-2024

Accepted: 05-11-2024

Abstract:

Introduction: For patients diagnosed with oral squamous cell carcinoma (OSCC), determining whether the tumor has penetrated the bone is crucial for therapy planning and surgical procedures. Computed Tomography (CT) imaging is preferred by radiologists due to its high sensitivity and specificity in detecting bone invasion.

Objectives In this study, we present a deep learning-based Convolutional Neural Network (CNN) model, optimized using a genetic algorithm, to automatically detect bone invasion in OSCC cases.

Methods: First, CT-scan images were collected from S. M.S. hospital, Jaipur and annotated by the hospital's experts. Further, all the collected images were changed from Digital Imaging and Communications in Medicine format (DICOM) to Portable Network Graphics (PNG) format as DICOM is very bulky to handle. Finally, GA is used to hyper-tune CNN parameters to get a good CNN architecture. The proposed model is compared with standard models like VGG16, VGG19, ResNet-50, MobileNetV2, DenseNet-121, and ResNet-101.

Results: The proposed model achieved a classification accuracy of 95.6%, outperforming six state-of-the-art transfer learning models, including VGG16, VGG19, ResNet-50, MobileNetV2, DenseNet-121, and ResNet-101.

Conclusions: The results demonstrate the effectiveness of our model in improving bone invasion detection accuracy, providing a valuable tool for clinical decision-making.

Keywords: Oral cancer, Bone Invasion, Convolution neural network, Genetic algorithm

1. Introduction

Cancer is the term for any unchecked proliferation of cells that intrudes on other tissue and harms it. An odd, small growth or sore that affects the lips, cheeks, sinuses, tongue, hard and soft palate, and the region between the base of the mouth and the oropharynx develops in the mouth. The initial indication of oral cancer is this. The sixth most prevalent form of cancer in the world is oral cancer. India is the country with the highest number of cases and one-third of the world's mouth cancer cases. Oral cancer is a serious health hazard for nations undergoing economic change. India records about 77,000 new cases and 52,000 fatalities annually or about one-fourth of all cases worldwide [1]. This

data is according to a 2020 study, and therefore proves that oral cancer is a very prevalent issue in India. The cancer occurs in the buccal area of the mouth. Squamous cells in the oral cavity are the first to develop into oral cancer. When the DNA of normal squamous cells changes and the cells start proliferating, the cells turn malignant. These malignant cells can travel to other parts of your mouth, your head, your neck, and even other parts of your body over time [2]. A variety of symptoms, such as recurring sores, lumps, or discoloured patches in the mouth or throat, can indicate oral cancer. Additional symptoms include soreness, hoarseness, trouble speaking or swallowing, bleeding that is not explained, and ear pain. Concerning symptoms include jaw swelling, neck lumps, dental abnormalities, abrupt weight loss, and persistent foul breath. Prompt action requires early diagnosis of these indications [3]. Treatment for oral cancer involves the use of several imaging modalities. When imaging techniques are used appropriately, they aid in the understanding of the tumor's dissemination to distant organs or lymph nodes (LN) as well as the assessment of vascularity. Furthermore, imaging aids in TNM staging, resection planning, and treatment.

The TNM staging system was developed by the Union for International Cancer Control and the American Joint Committee on Cancer, which is now a commonly used staging approach for determining cancer stage. The TNM staging structure enhances future research, decision-making, and outcome prediction. As the name suggests, its three main components are the tumor (T), node (N), and metastasis (M).

Since the first TNM staging manual was published by the AJCC in 1977, the bone invasion has been considered essential to T4 staging [4]. The probability of distant metastases and treatment failure is strongly correlated with bone involvement [5]. In addition to being crucial for staging, the identification of bone invasion in OSCC is also crucial for treatment planning. Consequently, a low assessment of bone involvement or overestimating this risk can result in needless excision and treatment, whereas involvement may cause distant metastases and locoregional recurrence. OSCC cancers destroy surrounding bone regions in 12–88% of cases. The identification of bone involvement in OSCC patients is largely dependent on clinical inspection, which includes palpation and direct examination [4]. However, the aforementioned considerations highlighted the requirement for a precise imaging technique that can assist in identifying bone invasion in OSCC patients. Numerous imaging modalities, such as computed tomography (CT), magnetic resonance imaging (MRI), X-ray, positron emission tomography (PET), bone scanning, and ultrasonography (USG), are available to detect bone invasion. Each modality has benefits and drawbacks. However, the results of the CT scan technology are very important for the investigation of malignant tumors since radiologists may see both soft tissue and bone involvement in the same test. Furthermore, it can identify bone deterioration with a high sensitivity (96%) and specificity (87%) [7]. However, determining the presence of bone involvement in CT scans is almost as challenging as categorizing the images since radiologists find it difficult to see the tumor's slight bone degeneration with the naked eye. The risk of fatalities and needless biopsies can be decreased by promptly identifying bone involvement in CT scans and treating patients appropriately.

Therefore, to overcome these challenges, this paper proposes a model that uses CNN with Genetic Algorithm optimization that will be able to detect bone invasion in its early stages accurately, so that an appropriate treatment plan can be written out and executed to increase the survival chances of the

patient. The CNN model uses a custom CNN architecture, the convolutional layers of the CNN model architecture are followed by max-pooling to extract features. Non-linearity is introduced by activation functions such as ReLU or ELU. Dropout layers come after convolutional layers to reduce overfitting. For classification, flattening comes before dense layers, with dropout for regularization. It is trained using the Adamax optimizer and categorical cross-entropy loss, with early halting to avoid overfitting. All things considered, the model prevents overfitting while effectively learning and classifying picture patterns. After this Genetic Algorithm is used to optimize the performance of this model. CNN hyperparameters are optimized for image classification using the genetic method. A population of CNN configurations is used at first. After undergoing training and evaluation, the most accurate models are chosen to become parents. The following generation's progeny are produced by crossover and mutation. Higher-performing models are favored as this process is repeated. Finding the best CNN configurations for picture classification is the algorithm's goal.

The dataset is collected from S.M.S. Hospital Jaipur since there is no publicly available dataset for this purpose. Finally, a comparison is done between the performance of the proposed model and Transfer learning models.

2. Objectives

In this paper, the major objective is to automate the bone invasion detection task using deep learning methods.

1. CT images of patients are collected from SMS Hospital, Jaipur, as there is no publicly available dataset.
2. To design a CNN model to automate the bone invasion detection task
3. Hyper- Parameters of CNN are tuned with GA.
4. The proposed model is compared with standard models like VGG16, VGG19, ResNet-50, MobileNetV2, DenseNet-121, and ResNet-101.

3. Literature Survey

The study titled "Automated Detection and Classification of Oral Lesions Using Deep Learning for Early Detection of Oral Cancer" [8] utilized the MeMoSA® platform, which involved collecting annotated images from clinical experts worldwide. The researchers employed deep neural networks, specifically ResNet-101 and Faster R-CNN, for the detection and classification of oral lesions. The findings revealed that ResNet-101 achieved an F1 score of 87.07% for lesion identification, while Faster R-CNN scored 41.18% for detecting lesions requiring referral. These initial results demonstrated the potential of deep learning for automated oral lesion detection. However, the study did not extensively explore its limitations, suggesting that future research should investigate factors such as generalizability and biases in model performance.

In another study, "Automatic detection of oral cancer in smartphone-based images using deep learning for early diagnosis," [9] a retrospective approach introduced "center positioning" for smartphone-based oral image collection. The study used a medium-sized dataset with five disease categories and employed a resampling method to address image variability. The HRNet deep learning network was used for oral cancer detection. The proposed method achieved 83.0% sensitivity, 96.6% specificity, 84.3% precision, and 83.6% F1 score on 455 test images. "Center positioning" outperformed the

simulated "random positioning" method by 8% in F1 score, and resampling led to an additional 6% improvement. HRNet slightly surpassed other models in various metrics. The study did not extensively discuss potential limitations, indicating that future research should explore the generalizability and real-world applicability of the proposed method (SPIE Digital Library).

The study "DEEPORCD: Detection of Oral Cancer using Deep Learning" [10] enhanced oral cancer detection through digital processing, utilizing three techniques: bag histogram of oriented gradients, wavelet features, and Zernike Moment. The fuzzy particle swarm optimization algorithm (FPSO) selected optimal characteristics, and a Convolution Neural Network (CNN) was used for feature classification. The method combining ABC, FPSO, and CNN showed improved efficiency in oral cancer detection. However, the study did not extensively discuss its limitations, suggesting that future research should explore the generalizability and practical applicability of the proposed method (Journal of Physics).

A review titled "Accuracy of imaging methods for detection of bone tissue invasion in patients with oral squamous cell carcinoma" [11] assessed studies published from 1960 to 2012 in English, Spanish, or German from MEDLINE, SciELO, and ScienceDirect. The inclusion criteria compared CT, MRI, panoramic radiography, PET/CT, and CBCT for SCC-induced mandibular bone invasion against histopathology, extracting sensitivity and specificity data. Of 338 articles, five met the inclusion criteria. The tests showed high diagnostic accuracy, with sensitivity rates of 94% for MRI, 91% for CBCT, 83% for CT, and 55% for panoramic radiography. Specificity rates were 100% for CT, MRI, and CBCT, 97% for PET/CT, and 91.7% for panoramic radiography. Despite the low to moderate evidence quality and methodological drawbacks, the study consistently supported the effectiveness of current imaging methods for detecting SCC-induced mandibular bone invasion (BIR Publications).

Another systematic review, "Accuracy of the Cone Beam Computed Tomography in the Detection of Bone Invasion in Patients with Oral Cancer," [12] examined English studies published from 1990 to 2017 in PubMed. This review analyzed CBCT's diagnostic accuracy for detecting bone tissue invasion by OSCC compared to other imaging methods. The review calculated sensitivity, specificity, LR+, LR-, diagnostic accuracy, and predictive values. Seven studies met the criteria, evaluating CT, MRI, CBCT, SPECT, MSCT, and PR. CBCT showed a significant LR+ value of 27.8 and promising predictive values ranging from 80.05% to 89.83% for detecting bone invasion by OSCC. The review highlighted the weak scientific evidence and underscored the necessity for future studies with a consistent methodological approach to better understand CBCT's impact on clinical decision-making (National Library of Medicine).

4. Dataset Collection

The dataset for this study was provided by the Sawai Man Singh (SMS) Hospital in Jaipur, India. A retrospective analysis was conducted on a total of 1755 CT scan images from 36 individuals between July 15, 2020, and April 30, 2021. Figure 1 shows some examples of pictures. Figures 1(a)–1(c) display images with bone invasion, whereas Figures 1(e)–1(g) display examples without bone invasion. The patients' genders differ greatly from one another. There were 4 (11%) female patients and 32 (89%) male patients in the dataset of 36 individuals, with a mean age of 43.95 years. Nineteen patients had bone invasion as shown by 915 CT images out of 1755 shots, while seventeen patients had no bone

invasion as shown by 840 images. Most occurrences of bone invasion were at a more advanced stage. Of the 19 patients with bone invasion, no cases were in the T1 or T2 stages; 15 (79%) were in the clinical T3 stage, and 4 (21%) were in the T4 stage. Excluded from consideration are cases in which bone loss was revealed by CT scans for other causes, such as age, fractures, rheumatoid arthritis, chronic kidney illness, etc. Every CT scan is histologically verified and categorized into the appropriate groups.

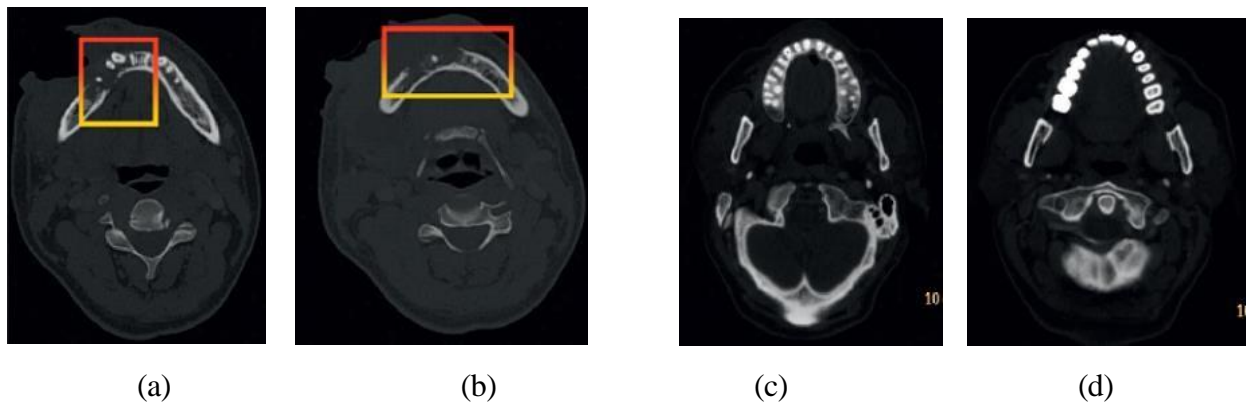


Figure 1: Image samples of OSCC patients (Labels: (a, b) with BI, (d, e) without BI)

For CT exams, a 128-slice Philips Ingenuity CT scanner is employed. CT scans with contrast were obtained by injecting 300 mg of IOHEXOL into the patients. The thickness of each slice was 1.55 mm, and the space between them was 0.75 mm. Every image was captured in an axial plane at a resolution of 1183×1067 pixels using the dicom format. The proportion of people with OSCC in different oral cavity regions is displayed in Table 2. Of all the photos gathered, 4 (21%) showed the caputinous mucosa, 14 (74%) the caputinous mucosa, and 1 (5%), the caputinous lip.

5. Methods

The research utilized a collection of bone invasion-demarcating oral cancer photos that were obtained from credible healthcare establishments. Preprocessing methods such as augmentation and scaling were used. Using Keras and TensorFlow, a unique CNN architecture with batch normalization and dropout layers was created. During the Google Colab training phase, the Adam optimizer and binary cross-entropy loss were employed. Hyperparameters were optimized using Genetic Algorithms. Standard metrics and comparisons against baselines were part of the model evaluation process. (See Figure 2)

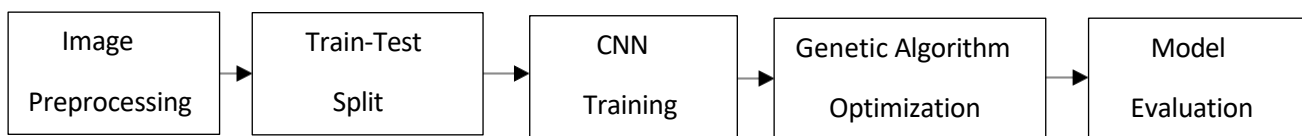


Figure 2: Flow diagram of proposed model

5.1. Image Preprocessing

In this project, reading a CSV file with image paths and labels is the first step in the image preparation process. Every image is transformed into arrays after being shrunk to a predetermined size of 28 by 28

pixels with three RGB colour channel. Standardized pixel values fall between 0 and 1 to ensure consistent input to the model. Pre-processing methods such as augmentation and scaling were used.

5.2. Train – Test Split

The dataset is divided into training and testing sets in the train-test split process, with 40% of the data going toward testing and 60% going toward training. Furthermore, 20% of the original dataset is converted into a validation set using the training data in order to help with hyperparameter tweaking and avoid overfitting.

5.3 Training

This model requires the completion of numerous crucial phases during training. Using the Keras Sequential API, a convolutional neural network (CNN) architecture is first defined. The design is made up of several layers. To extract features from the input images, max-pooling is placed after two convolutional layers. To reduce overfitting, dropout layers are used, which randomly deactivate a portion of neurons during training. The output is then flattened and classified using fully linked dense layers, where non-linearity is introduced using activation functions. The model architecture is built using the categorical cross-entropy loss function, Adamax optimizer, and accuracy metric once it has been defined. The model is now prepared to be trained with the provided training set. The CNN model uses a custom CNN architecture, the convolutional layers of the CNN model architecture are followed by max-pooling to extract features. Non-linearity is introduced by activation functions such as ReLU or ELU. Dropout layers come after convolutional layers to reduce overfitting. For classification, flattening comes before dense layers, with dropout for regularization. It is trained using the Adamax optimizer and categorical cross-entropy loss, with early halting to avoid overfitting. All things considered, the model prevents overfitting while effectively learning and classifying picture patterns. After this Genetic Algorithm is used to optimize the performance of this model. CNN hyperparameters are optimized for image classification using the genetic method. A population of CNN configurations is used at first. After undergoing training and evaluation, the most accurate models are chosen to become parents. The following generation's progeny are produced by crossover and mutation. Higher-performing models are favored as this process is repeated. Finding the best CNN configurations for picture classification is the algorithm's goal.

5.4 Genetic Algorithm Optimization

Natural selection and genetics serve as the inspiration for the heuristic search method used in this project's genetic algorithm optimization procedure. First, a population of potential fixes, called chromosomes, is created at random. A convolutional neural network (CNN) model's setup for image classification is the optimization problem in this example, and each chromosome represents a possible solution.

The genetic algorithm investigates and evolves the population of chromosomes over several generations by a process of crossover, mutation, and selection. Chromosomes with higher fitness values are more likely to be selected as parents during selection in order to produce offspring. In order to create new child chromosomes through crossover, genetic material from two parent chromosomes is combined, simulating the process of reproduction and genetic recombination in natural evolution.

Individual chromosomes might undergo random alterations due to mutations, which opens up new search space.

Iteratively, the evolutionary process continues for a predetermined number of generations or until the target performance level is attained. The population changes during the optimization process, and the most suitable individuals (chromosomes) are kept for additional research. The evolutionary method aims to find an optimal or nearly ideal solution to the CNN model configuration problem for image classification by iteratively improving the population through selection, crossover, and mutation.

5.5 Model evaluation

The classification report also includes an extensive analysis of multiple classification characteristics, such as precision, recall, F1-score, and support for each class. A classification report, a confusion matrix, and kappa score is drawn to assess the model's performance.

6. Results

This section details the classification results given by the proposed model.

6.1 Classification report

The classification report also includes an extensive analysis of multiple classification characteristics, such as precision, recall, F1-score, and support for each class (See Table 1) .

$$Accuracy = (Total\ Number\ of\ Predictions)/(Number\ of\ Correct\ Predictions)$$

$$Precision = (True\ Positives + False\ Positives)/(True\ Positives)$$

$$Recall = (True\ Positives)/(True\ Positives + False\ Negatives)$$

Learning models	Accuracy	F1-score	Precision	Recall	AUC-score
VGG-16	87.87	84.62	85.33	83.39 81.44	86.7
	85.95	82.12 78.33	82.9	77.4	87.29
	83.19		79.51		84.42
VGG-19		57.88		57.56 80.33	
	70.79	79.78 80.46	60.86	79.46 68.87	72.04
	84.47 84.84	70.54 51.8	79.3	52.88	86.01
	78.78 68.87		81.73 74.35		85.64
			55.22		83.23
					70.47
ResNet-50	83.47 79.33	79.66 70.83	79.33 75.58	80.03 68.95	84.82
	84.29 85.67	79.88 82.27	80.86 82.08	79.08 82.47	86.87
MobileNet	84.16 81.54	79.23 76.35	80.45 77.22	79	89.95
	82.92	77.43 64.89	79.6	75.65 75.99	90.1
	76.3		71.1	63.5	88.95
					85.59

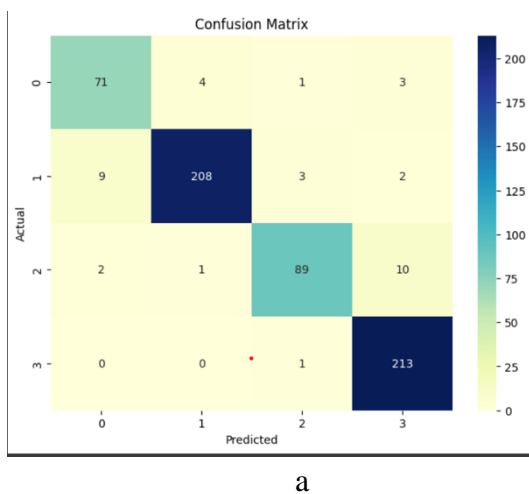
DenseNet121	82.65 83.98	82.01 83.61	83.58 83.31	81.13 84.18	89
	84.43 78.51	75.3 78.61	83.42 78.31	72.1	80.64
				79.12	
					89.18
					91.37
				94.5	
				90.12	
ResNet101	79.25 78.09	76.37 69.13	75.32 70.31	82.69 68.28	88.9
	76.08	74.18 77.02	75.17 75.54	83.17	89.45
	80.4			81.9	87.21
					88.5
CNN with GA optimization	0.94	0.88	0.87	0.90	0.952
		0.96	0.98	0.94	
		0.91	0.95	0.87	
		0.96	0.93	1.00	

Table 1. Comparing the performance metrics of the current model to Transfer learning models

6.2 Confusion Matrix and Kappa score

The confusion matrix facilitates a comprehensive examination of classification performance across several classes by offering a tabular depiction of actual versus projected class labels. It helps to understand the behaviour of the model by making it possible to distinguish between true negatives, false negatives, and true positives (See Figure 3 (a)).

Kappa score, which calculates the agreement between expected and actual class labels while considering chance agreement, is employed to assess the model's performance. A better agreement between the anticipated and actual class labels is indicated by a higher Kappa value; a score of 1 denotes perfect agreement, while a score of 0 denotes agreement as random as chance (See Figure 3 (b)).



Model	Kappa Coefficient
CNN model with GA optimization	0.9
ResNet-101	0.55
DenseNet-121	0.5
ResNet-50	0.45
Vgg-19	0.5
MobileNetV2	0.35
Vgg-16	0.2

Figure 3: Confusion matrix (a) and kappa score (b) of proposed model

6.3 Results given by GA optimizer

Table 2 represents the results generated after 3 generations. In generation 3 desired accuracy meets with the obtained accuracy, i.e. 95.6%.

GENERATION 1	
PARENT 1	{'f1': 64, 'f2': 64, 'f3': 512, 'k': 3, 'a1': 'relu', 'a2': 'relu', 'd1': 0.3, 'd2': 0.1, 'op': 'adamax', 'ep': 51}
PARENT 2	{'f1': 32, 'f2': 128, 'f3': 256, 'k': 3, 'a1': 'elu', 'a2': 'selu', 'd1': 0.2, 'd2': 0.3, 'op': 'adam', 'ep': 54}
MAX. ACCURACY IN GENERATION 1	0.948
GENERATION 2	
PARENT 1	{'model': <keras.src.engine.sequential.Sequential object at 0x7ca6ef6eb160>, 'f1': 64, 'f2': 64, 'f3': 512, 'k': 3, 'a1': 'relu', 'a2': 'relu', 'd1': 0.3, 'd2': 0.3, 'op': 'adam', 'ep': 54}
PARENT 2	{'f1': 64, 'f2': 64, 'f3': 128, 'k': 5, 'a1': 'relu', 'a2': 'selu', 'd1': 0.1, 'd2': 0.2, 'op': 'adamax', 'ep': 59}
MAX. ACCURACY IN GENERATION 2	0.948
GENERATION 3	
PARENT 1	{'model': <keras.src.engine.sequential.Sequential object at 0x7ca6f2823e50>, 'f1': 64, 'f2': 64, 'f3': 512, 'k': 3, 'a1': 'relu', 'a2': 'relu', 'd1': 0.3, 'd2': 0.3, 'op': 'adam', 'ep': 54}
PARENT 2	{'f1': 64, 'f2': 64, 'f3': 512, 'k': 3, 'a1': 'relu', 'a2': 'relu', 'd1': 0.3, 'd2': 0.1, 'op': 'adamax', 'ep': 51}
MAX. ACCURACY IN GENERATION 3	0.956
OBTAINED THE DESIRED ACCURACY	0.956

Table 2: Results given by GA optimized CNN for 3 generations

7. Discussion

In medical imaging, deep learning algorithms are becoming increasingly popular because they provide precise and affordable results. This paper employs a DL-based framework to identify bone invasion in cases of oral squamous cell carcinoma (OSCC) using CT scan data. Experts classified the dataset, which included CT pictures of patients with oral cancer, which was gathered from SMS Hospital in Jaipur, India. The goal of experimenting with different CNN settings was to set up the ideal CNN model. The suggested model, which was trained using an optimization strategy based on genetic algorithms, was evaluated in terms of performance against six common Transfer Learning (TL) models. With a kappa score of 91.7% and a roc_auc of 95.2%, the results show that our improved

model achieves impressive accuracy. Following optimization using a genetic algorithm, the model's accuracy is 95.6%. The little loss the model produces shows how robust it is. The model's high AUC value of 95.6% provides additional validation for its efficacy. The capabilities of our model are significant because accurate tumor staging and treatment planning in OSCC depend on prompt identification of bone invasion. Future studies can address the limitations of the dataset, which include the lack of cases connected to other characteristics like age, fractures, and chronic conditions.

References:

- [1] V. Borse, A. N. Konwar, and P. Buragohain, "Oral cancer diagnosis and perspectives in India," *Sens Int*, vol. 1, p. 100046, 2020, doi: 10.1016/j.sintl.2020.100046.
- [2] S. Langmaid, "An Overview of Oral Cancer," WebMD. Accessed: May 14, 2024. [Online]. Available: <https://www.webmd.com/oral-health/oral-cancer>
- [3] "Oral Cancer: Causes, Symptoms & Treatment," Cleveland Clinic. Accessed: May 14, 2024. [Online]. Available: <https://my.clevelandclinic.org/health/diseases/11184-oral-cancer>
- [4] F. De Felice *et al.*, "Treatment improvement and better patient care: which is the most important one in oral cavity cancer?," *Radiation Oncology*, vol. 9, pp. 1–7, 2014.
- [5] A. Ebrahimi, R. Murali, K. Gao, M. S. Elliott, and J. R. Clark, "The prognostic and staging implications of bone invasion in oral squamous cell carcinoma," *Cancer*, vol. 117, no. 19, pp. 4460–4467, Oct. 2011, doi: 10.1002/cncr.26032.
- [6] M. A. P. Albuquerque, M. E. Kuruoshi, I. R. S. Oliveira, and M. G. P. Cavalcanti, "CT assessment of the correlation between clinical examination and bone involvement in oral malignant tumors," *Braz. oral res.*, vol. 23, no. 2, pp. 196–202, Jun. 2009, doi: 10.1590/S1806-83242009000200017.
- [7] S. K. Mukherji, D. L. Isaacs, A. Creager, W. Shockley, M. Weissler, and D. Armao, "CT Detection of Mandibular Invasion by Squamous Cell Carcinoma of the Oral Cavity," *American Journal of Roentgenology*, vol. 177, no. 1, pp. 237–243, Jul. 2001, doi: 10.2214/ajr.177.1.1770237.
- [8] R. A. Welikala *et al.*, "Automated Detection and Classification of Oral Lesions Using Deep Learning for Early Detection of Oral Cancer," *IEEE Access*, vol. 8, pp. 132677–132693, 2020, doi: 10.1109/ACCESS.2020.3010180.
- [9] H. Lin, H. Chen, L. Weng, J. Shao, and J. Lin, "Automatic detection of oral cancer in smartphone-based images using deep learning for early diagnosis," *J. Biomed. Opt.*, vol. 26, no. 08, Aug. 2021, doi: 10.1117/1.JBO.26.8.086007.
- [10] R. Dharani and S. Revathy, "DEEPORCD: Detection of Oral Cancer using Deep Learning," *J. Phys.: Conf. Ser.*, vol. 1911, no. 1, p. 012006, May 2021, doi: 10.1088/1742-6596/1911/1/012006.
- [11] S. Uribe, L. Rojas, and C. Rosas, "Accuracy of imaging methods for detection of bone tissue invasion in patients with oral squamous cell carcinoma," *Dentomaxillofacial Radiology*, vol. 42, no. 6, p. 20120346, Jun. 2013, doi: 10.1259/dmfr.20120346.
- [12] G. P. Bombeccari, V. Candotto, A. B. Gianni, F. Carinci, and F. Spadari, "Accuracy of the Cone Beam Computed Tomography in the Detection of Bone Invasion in Patients with Oral Cancer: A Systematic Review," *Eurasian J Med*, vol. 51, no. 3, pp. 298–306, Oct. 2019, doi: 10.5152/eurasianjmed.2019.18101.
- [13] K. Warin, W. Limprasert, S. Suebnukarn, S. Jinaporntham, and P. Jantana, "Automatic classification and detection of oral cancer in photographic images using deep learning algorithms," *J Oral Pathology Medicine*, vol. 50, no. 9, pp. 911–918, Oct. 2021, doi: 10.1111/jop.13227.